

Corrugations and Spirals: Recent Disturbances in Saturn's D ring

M. Hedman (1), M. Showalter (2) and J.A. Burns (3)

(1) University of Idaho, Moscow, Idaho, USA, (2) SETI Institute, Mountain View, California, USA, (3) Cornell University, Ithaca, New York, USA (mhedman@uidaho.edu)

Abstract

The D ring is Saturn's innermost ring, extending between 65,000 and 74,950 km from Saturn's center. It is also an extremely dynamic ring, exhibiting a number of structures that vary substantially over time scales of a few years to decades. One particularly interesting class of time-variable features found in this ring are highly periodic variations in the ring's brightness with radial wavelengths that become progressively shorter over time. These patterns are most likely due to some event in the recent past that disturbed the rings and produced organized non-circular motions in the ring-particles' orbits. Indeed, similar features in Jupiter's rings appear to have been generated in 1994 when debris from Shoemaker-Levy 9 passed through the rings [?]. These patterns can therefore provide new insights into the rings' recent history. More specifically, one set of patterns may have been generated by a cometary impact in 1983, and detailed examinations of these structures provide constraints on the possible trajectory of the impacting debris. Meanwhile, another pattern appeared in the D ring a few years ago that could have been generated by either another impact or by some disturbance in Saturn's electromagnetic environment.

1. New Information about what happened to Saturn in 1983

Previous investigations of Saturn's outer D ring (73,200-74,000 km from Saturn's center) identified periodic brightness variations whose radial wavenumber increased linearly over time [?]. These brightness variations appeared to be due to a vertical corrugation, and later observations revealed that a similar corrugation extended across the entire C ring [?]. These patterns could be explained if some event like a cometary impact caused the ring to become tilted relative to the planet's equator plane in 1983. Differential nodal regression then transformed this tilted ring into a cor-

rugated ring with the radial wavelengths we observe today. Additional Cassini observations of these structures now reveal that the outer D ring is not only corrugated, but also contains a time-variable periodic modulation in its optical depth that probably represents organized eccentric motions of the D-ring's particles [?]. This second pattern suggests that whatever event tilted the rings also disturbed the radial or azimuthal velocities of the ring particles. Furthermore, the relative amplitudes of the two patterns indicate that the vertical motions induced by the 1983 event were about a factor two times larger than the corresponding in-plane motions. If these structures were indeed produced by an impact, material would need to strike the ring at a steep angle ($> 60^\circ$ from the ring plane) to produce such motions. Also, the corrugation wavelengths in the D ring are about 0.7% shorter than one would predict based on extrapolations from similar structures in the nearby C ring. This could indicate that the D-ring was tilted/disturbed about 60 days before the C ring. Such a timing difference could be explained if the material that struck the rings was derived from debris released when some object broke up near Saturn some months earlier. To reproduce the observed time difference, this debris would need to have a substantial initial velocity dispersion and then have its orbital properties perturbed by some phenomenon like solar tides prior to its collision with the rings.

2. A new pattern in the inner D ring

Images obtained by the Cassini spacecraft between 2012 and 2014 reveal periodic brightness variations in the inner D ring (69,000-71,000 km from Saturn's center), a region that had previously appeared to be rather featureless. The radial wavenumber of this pattern has decreased steadily with time since it was first observed, and it appears to be another pattern created by some event that disturbed the orbital motions of the ring particles. The observed trends in the pattern's radial wavenumber indicate that the ring-

disturbing event occurred in early December, 2011. Similar events in 1979 may have generated the periodic patterns seen in this same region by the Voyager spacecraft. The 2011 event could have been caused by debris striking the rings, or by some sort of disturbance in the planet's electromagnetic environment. The rapid reduction in the intensity of the brightness variations over the course of the last two years indicate that some as-yet unidentified process is quickly dissipating organized epicyclic motions in this region.

References

- [1] M.R. Showalter, M.M. Hedman, J.A. Burns. The Impact of comet Shoemaker-Levy 9 sends ripples through the rings of Jupiter. *Science* 332:711-713 2011.
- [2] M.M. Hedman, J.A. Burns, M.R. Showalter, C.C. Porco, P.D. Nicholson, A.S. Bosh, M.S. Tiscareno, R.H. Brown, B.J. Buratti, K.H. Baines, R.N. Clark. Saturn's dynamic D ring. *Icarus* 188:89-107 2007.
- [3] M.M. Hedman, J.A. Burns, M.W. Evans, M.S. Tiscareno, C.C. Porco. Saturn's curiously corrugated C ring. *Science* 332:708-711 2011.
- [4] M.M. Hedman, J.A. Burns, M.R. Showalter. Corrugations and eccentric spirals in Saturn's D ring: New insights into what happened at Saturn in 1983 *Icarus* 248:137-161 2015.

Non-Linear Dynamics of Saturn's Rings

L.W. Esposito

Laboratory for Atmospheric and Space Physics, Univ. of Colorado, 3665 Discovery Dr. Boulder CO 80303(larry.esposito@lasp.colorado)

Non-linear processes can explain why Saturn's rings are so active and dynamic.

Ring systems differ from simple linear systems in two significant ways:

1. They are systems of granular material: where particle-to-particle collisions dominate; thus a *kinetic*, not a *fluid* description needed. We find that stresses are strikingly inhomogeneous and fluctuations are large compared to equilibrium.
2. They are strongly forced by resonances: which drive a non-linear response, pushing the system across thresholds that lead to persistent states.

Some of this non-linearity is captured in a simple Predator-Prey Model:

Periodic forcing from the moon causes streamline crowding; This damps the relative velocity, and allows aggregates to grow. About a quarter phase later, the aggregates stir the system to higher relative velocity and the limit cycle repeats each orbit, with relative velocity ranging from nearly zero to a multiple of the orbit average: 2-10x is possible.

Results of driven N-body systems by Stuart Robbins: Even unforced rings show large variations; Forcing triggers aggregation; Some limit cycles and phase lags seen, but not always as predicted by predator-prey model.

Summary of Halo Results: A predator-prey model for ring dynamics produces transient structures like 'straw' that can explain the halo structure and spectroscopy:

Cyclic velocity changes cause perturbed regions to reach higher collision speeds at some orbital phases, which preferentially removes small regolith particles; Surrounding particles diffuse back too slowly to erase the effect: this gives the halo morphology; This requires energetic collisions ($v \approx 10\text{m/sec}$, with throw distances about 200km, implying objects of scale $R \approx 20\text{km}$); We propose 'straw'.

Transform to Duffing Eqn : With the coordinate transformation, $z = M^{2/3}$, the Predator-Prey equations can be combined to form a single second-order differential equation with harmonic resonance forcing.

Ring dynamics and history implications: Moon-triggered clumping at perturbed regions in Saturn's rings creates both high velocity dispersion and large aggregates at these distances, explaining both small and large particles observed there. This confirms the triple architecture of ring particles: a broad size distribution of particles; these aggregate into temporary rubble piles; coated by a regolith of dust. Aggregates can explain many dynamic aspects of the rings and can renew rings by shielding and recycling the material within them, depending on how long the mass is sequestered. We can ask: Are Saturn's rings a *chaotic* non-linear driven system?

Dust Impact Detection by the Cassini Langmuir Probe in Saturn's E ring

H.-W. Hsu (1), J.-E. Wahlund (2), M. Morooka (1), S. Kempf (1), and M. Horányi (1)

(1) LASP, Uni. of Colorado, Boulder, CO, USA, (2) Swedish Institute of Space Physics, Uppsala, Sweden

Abstract

In this work, we present preliminary analysis of dust impact detections recorded by the Cassini Langmuir probe (LP) in Saturn's E ring. These signals appear as sharp spikes in the LP current-voltage (I-V) curves and show clear correlation with the E ring dust density. The statistical analysis will help to understand the nature of these detections as well as provide an alternative method to study the densest part of the E ring.

1. Introduction

Individual examination reveals the existence of sharp spikes in the Cassini Radio and Plasma Wave Science / Langmuir probe (RPWS/LP) I-V sweeps. They are characterized as a sudden increase or decrease in the probe current, with many of them appearing as one-point anomalies lasting less than a millisecond. Their occurrence generally correlates with the E ring dust density - the closer to the ring plane and Enceladus, the more frequent the appearance of spikes. Considering these characteristics, these signals are thought to be caused by dust impacts - most likely the collection of plasma produced from dust-probe impacts. Because of the low detection rate and the flexibility regarding to the spacecraft attitude, LP spikes provide an alternative way to explore the densest part of the E ring.

2. This Work

In this work we will present preliminary statistical analysis of the LP spike appearance as a function of the spacecraft location, the relative dust speed, the spacecraft and probe potentials, and other relevant parameters. Comparison with measurements carried out by the High Rate Detector, a subsystem of the Cassini Cosmic Dust Analyser, will provide constraints on the dust grain size responsible for these detections. We will also examine their spatial distribution to identify features that may associate with ring dynamical ef-

fects, such as the seasonal variation or the noon-to-midnight electric field.

3. Figure

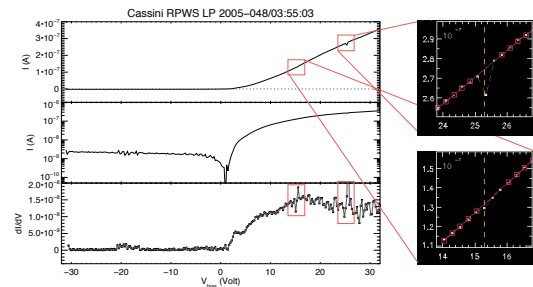


Figure 1: An example of the Cassini Langmuir probe dust impact detection. Two spikes occurred in one single I-V curve (i.e., recorded within 0.5 second). The spacecraft was in the ring plane at $4.1R_S$ (R_S is radius of Saturn) distance to Saturn. It is not clear if the higher amplitude of the spike registered at +25V probe bias potential (ϕ_{bias}) is caused by a larger/fast impactor or a higher collection efficiency at higher ϕ_{bias} .

Exogenous dust delivery into the Saturnian system and the age of Saturn's rings

S. Kempf (1), M. Horanyi (1), R. Srama (2) and N. Altobelli (3)

(1) LASP, University of Colorado at Boulder, Boulder, USA (sascha.kempf@lasp.colorado.edu) (2) IRS, Stuttgart University, Stuttgart, Germany (3) ESA, ESAC, Spain

Abstract

Even 450 years after Galileo Galilei's discovery of Saturn's rings, their origin and evolution is still not known. The rings are the brightest of the four ring systems of the solar system and have at least the mass of the moon Mimas[?]. Interactions with Saturn's moons and viscous spreading of the ring material seem to imply a ring age of about a tenth of the age of the Saturnian system of about 4.5 billion years[?, ?]. A young ring age is problematic because the disruption of a Mimas-sized body or a comet in the Roche zone of Saturn would result in a ring with a much larger rock content than observed today[?, ?, ?]. The unique ring color resulting mainly from the pollution of the ring material with interplanetary meteoroids provides a key for constraining the ring age[?, ?, ?].

Here we report on the first direct measurements of the meteoroid flux into the Saturnian system by Cassini's Cosmic Dust Analyzer (CDA). We measured the impact speed vectors of 133 extrinsic micrometeoroids $\geq 2\mu\text{m}$ and determined their orbital elements. We determined the mass flux into the Saturnian system to be $10^{-18}\text{kg/m}^2\text{s}$. This finding suggests a ring exposure time of 4.5 billion years and is in support of an early ring generation from a proto-Titan during the formation of the Saturnian system[?].

References

- [1] Esposito, L. W., Ocallaghan, M. & West, R. A. The structure of Saturn's rings - Implications from the Voyager stellar occultation. *Icarus***56**, 439–452 (1983).
- [2] Charnoz, S., Dones, L., Esposito, L. W., Estrada, P. R. & Hedman, M. M. *Origin and Evolution of Saturn's Ring System*, 537 (Springer, 2009).
- [3] Cuzzi, J. N. *et al.* An Evolving View of Saturn's Dynamic Rings. *Science* **327**, 1470– (2010).
- [4] Lissauer, J. J., Squyres, S. W. & Hartmann, W. K. Bombardment history of the Saturn system. *Jour. Geophys. Res.* **93**, 13776–13804 (1988).
- [5] Charnoz, S., Morbidelli, A., Dones, L. & Salmon, J. Did Saturn's rings form during the Late Heavy Bombardment? *Icarus* **199**, 413–428 (2009).
- [6] Dones, L. A recent cometary origin for Saturn's rings? *Icarus***92**, 194–203 (1991).
- [7] Durisen, R. H. Particle erosion mechanisms and mass redistribution in Saturn's rings. *Advances in Space Research* **4**, 13–21 (1984).
- [8] Durisen, R. H., Bode, P. W., Cuzzi, J. N., Cederbloom, S. E. & Murphy, B. W. Ballistic transport in planetary ring systems due to particle erosion mechanisms. II - Theoretical models for Saturn's A- and B-ring inner edges. *Icarus* **100**, 364–393 (1992).
- [9] Cuzzi, J. N. & Estrada, P. R. Compositional Evolution of Saturn's Rings Due to Meteoroid Bombardment. *Icarus* **132**, 1–35 (1998).
- [10] Canup, R. M. Origin of Saturn's rings and inner moons by mass removal from a lost Titan-sized satellite. *Nature* **468**, 943–926 (2010).

Hydrodynamic simulations of propellers: Isothermal model

M. Seiß, H. Hoffmann and F. Spahn

Department of Physics and Astronomy, University of Potsdam, Germany (martins@agnld.uni-potsdam.de)

Abstract

Small moons embedded in Saturn's rings can cause S-shaped density structures, called propellers, in their close vicinity. These structures have been predicted first on the basis of a combined model involving gravitational scattering of test particles (creating the structure) and diffusion (smearing out the structure) [1, 2]. The propeller model was confirmed later with the help of N-body simulations showing the additional appearance of moon wakes adjacent to the S-shaped gaps [3, 4]. It was a great success of the Cassini mission when the propeller was detected in the ISS imaging [5, 6] and UVIS occultation data [7].

Here we present an isothermal hydrodynamic simulation of a propeller as a further development of the original model [1, 2] where gravitational scattering and diffusion had to be treated separately. With this new approach we prove the correctness of the predicted scaling laws for the radial and azimuthal extent of the propeller. Furthermore, we will show a comparison between results of N-body and hydrodynamic simulations. Finally, we will present simulation results of the giant propeller Bleriot, which can not be modeled by N-body simulations in its full extent yet.

Acknowledgements

This work was supported by Deutsches Zentrum für Luft- und Raumfahrt (OH 1401) and by Deutsche Forschungsgemeinschaft (Sp 384/24-2).

References

- [1] F. Spahn and M. Sremčević, "Density patterns induced by small moonlets in Saturn's rings?," *Astronomy and Astrophysics*, vol. 358, pp. 368–372, June 2000.
- [2] M. Sremčević, F. Spahn, and W. J. Duschl, "Density structures in perturbed thin cold discs," *Monthly Notices Royal Astron. Soc.*, vol. 337, pp. 1139–1152, Dec. 2002.
- [3] M. Seiß, F. Spahn, M. Sremčević, and H. Salo, "Structures induced by small moonlets in Saturn's rings: Implications for the Cassini Mission," *Geophysical Research Letters*, vol. 32, p. 11205, June 2005.
- [4] M. C. Lewis and G. R. Stewart, "Features around embedded moonlets in Saturn's rings: The role of self-gravity and particle size distributions," *Icarus*, vol. 199, pp. 387–412, Feb. 2009.
- [5] M. S. Tiscareno, J. A. Burns, M. M. Hedman, C. C. Porco, J. W. Weiss, L. Dones, D. C. Richardson, and C. D. Murray, "100-metre-diameter moonlets in Saturn's A ring from observations of 'propeller' structures," *Nature*, vol. 440, pp. 648–650, Mar. 2006.
- [6] M. Sremčević, J. Schmidt, H. Salo, M. Seiß, F. Spahn, and N. Albers, "A belt of moonlets in Saturn's A ring," *Nature*, vol. 449, pp. 1019–1021, Oct. 2007.
- [7] K. Baillié, J. E. Colwell, L. W. Esposito, and M. C. Lewis, "Meter-sized Moonlet Population in Saturn's C Ring and Cassini Division," *Astronomical Journal*, vol. 145, p. 171, June 2013.

The dust environment surrounding the E-ring moons Dione, Helene and Polydeuce

T. Moldenhawer, H. Hoffmann, M. Seiß, M. Sachse and F. Spahn
Institute of Physics and Astronomy, University of Potsdam, Germany (hohoff@uni-potsdam.de)

Abstract

Compared to the dust clouds around three of the Galilean satellites of Jupiter, no clear Saturnian pendants have been found yet by the CDA detector aboard the Cassini spacecraft. However, three dust tori and arcs have been detected along the orbits of Pallene, Methone and Anthe in ISS images [1] and the Pallene dust torus was confirmed by in situ CDA measurements [4]. These observations have sparked interest whether the small co-orbital companions to E-ring moons like Dione or Thetys are efficient dust sources.

We simulate the motion of dust particles, which originate from hypervelocity impacts of micrometeoroids onto Dione, Helene and Polydeuce [2]. Gravity, Lorentz force, solar radiation pressure and plasma drag are considered for the dynamic evolution of small dust particles. Assuming a steady state distribution, we scale the phase space data with dust production rates based on recent IDP measurements at Saturn [3]. We will present dust particle number densities along the orbits of Dione, Helene and Polydeuce and we will make predictions for the Cassini flybys of Helene and Polydeuce, which take place in the summer and fall this year.

dust clouds around planetary satellites: spherically symmetric case, *Planetary and Space Science*, 51, 251-269, 2003.

- [3] S. Kempf, N. Altobelli, M. Horanyi, and R. Srama: The mass flux of micrometeoroids into the Saturnian system. *European Planetary Science Congress 2014* (227).
- [4] Seiß, M., Srama, R., Kempf, S., Sun, K.-L., Seiler, M., Moragas-Klostermeyer, G., and Spahn, F.: Pallene dust torus observations by the Cosmic Dust Analyzer. *European Planetary Science Congress 2014* (375).

Acknowledgements

This work was supported by Deutsche Forschungsgemeinschaft (Sp 384/24-2) and by Deutsches Zentrum für Luft- und Raumfahrt (OH 1401).

References

- [1] Hedman, M. M., Murray, C. D., et al.: Three tenuous rings/arcs for three tiny moons, *Icarus*, 199, 378-386, 2009.
- [2] Krivov, A. V., Sremčević, M., Spahn, F., Dikarev, V. V. and Kholshchevnikov, K. V.: Impact-generated

Calibration of the Cassini Cosmic Dust Analyzer

J. Simolka (1), R. Srama (1), T. Albin (1, 2), S. Bugiel (1), S. Kempf (3), Y. Li (1), G. Moragas-Klostermeyer (1), F. Postberg (4), H. Strack (1)

(1) Institute of Space Systems – Universität Stuttgart, Germany (2) Carl von Ossietzky Universität Oldenburg, Germany (3) University of Colorado at Boulder, USA (4) Universität Heidelberg, Germany
 (simolka@irs.uni-stuttgart.de / Fax: +49 711 685 63596)

Abstract

The Cosmic Dust Analyzer (CDA) onboard the Cassini spacecraft detects micron and sub-micron sized particles in the Saturn environment since 2004. The impact ionization based instrument measures the positive and negative charges of the impact plasma generated by striking particles. This signals yield the impact velocity and the particle mass. Therefore the instrument needs to be carefully calibrated. Calibration is performed utilizing the dust accelerator facility in Heidelberg which is able to accelerate micron and sub-micron sized dust particles to velocities relevant in space. Particles on circular orbits in Saturn's ring plane allow cross calibration of the dust telescope since their velocity and mass range is well known. However, since the initial calibration the scientific knowledge of the local dust environment has drastically improved (thanks to Cassini). At the same time laboratory testing facilities evolved over the years and allow a better recreation of actual conditions nowadays. Especially a larger variety of dust types particularly of mineral compositions is available nowadays.

1. Introduction

When a dust particle hits the detector target it gets partially or completely ionized. Furthermore – dependent on the impact velocity – the impact generates ejecta (particle and target fragments) which can cause secondary and even tertiary impacts. These events shape a plasma cloud which is separated by an electric field. Negative charges are collected at the target and positive charges at the ion collector. The target consists of two separate parts. The large target area of the impact ionization detector consists of a gold coated hemisphere with a diameter of 40 cm. The smaller chemical analyzer target is part of CDAs time of flight mass spectrometer. Figure 1 shows a schematic drawing of CDA and two impact events with correlating signals.

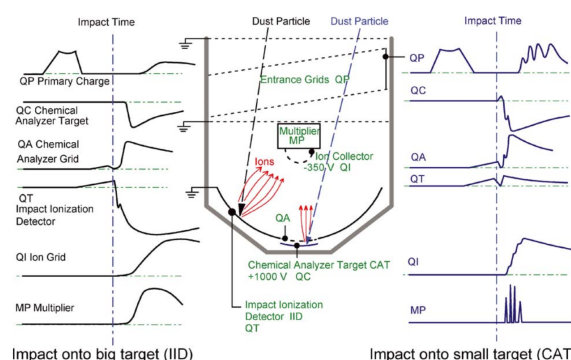


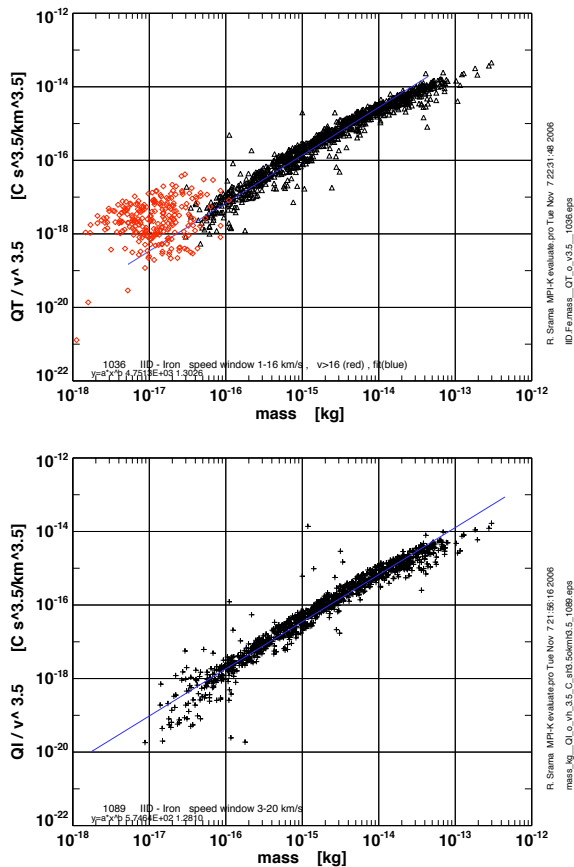
Figure 1: Schematics of CDA. Two exemplary impact events and their correlating signals are shown for an impact on the large target and on the chemical analyzer target. [3]

2. Particle Velocity and Mass Determination

For modeling Saturn's dust environment the size and velocity of the dust grains is of particular interest. These (and more) properties can be obtained from CDA's measurements.

2.1 Impact Velocity

Previous impact ionization detectors have shown a correlation of the charge signal rise times and the impact velocity – independent from the particle mass and impact angle. [1] CDA uses this phenomena to determine the velocity of striking particles (Further measurements and effects are considered for better accuracy). The rise time is defined by the time interval between 10% and 90% of the signal waveform's peak value. [3] The slight dependency of the particle composition is not considered in the current calibration model. The particle velocity can be derived from the impact velocity and the velocity of the spacecraft.



2.2 Particle Mass

There is a well known empirical relationship between the impact charge Q , impact velocity v and particle mass m . The amount of the generated impact plasma increases with higher particle mass and velocity.

$$Q \sim m^\alpha \cdot v^\beta \quad (1)$$

Direct measurement of the impact charge and determination of the impact velocity cf. 2.1 yield the particle mass.

Figure 2 shows the ratio $Q/v^{3.5}$ over the particle mass m for measurements taken in the laboratory. The upper graph corresponds to negative charges measured at the target while the lower graph reflects the positive charge measurements at the ion collector. The red symbols in the upper graph correlate with impact events with a velocity > 16 km/s indicating a regime where no secondary impacts occur. [2] The speed exponent β is set to 3.5 which yields a clearly discernible

trend over the shown velocity range.

3. Summary and Conclusions

CDA is investigating the dust environment at Saturn for over a decade now. The collected data helped to obtain a better understanding of the local evolution of micron and sub-micron sized particles. One of the particles' interesting properties are their velocity and mass. The gained scientific knowledge and advanced laboratory facilities allow us to redefine the instruments calibration model. The poster presents the latest methods and an outlook into the recalibration of the cosmic dust analyzer.

References

- [1] J. R. Gröller, E. Grün: Calibration of the *GALILEO/ULYSSES* dust detectors with different projectile materials and at varying impact angles, Planetary and Space Science, Vol. 37, No 10, pp. 1197-1206, 1989.
- [2] R. Srama: Cassini-Huygens and Beyond – Tools for Dust Astronomy, Universität Stuttgart, 2009.
- [3] R. Srama: Vom Cosmic-Dust-Analyzer zur Modellbeschreibung wissenschaftlicher Raumsonden, Technische Universität München, 2000.

A Transiting Extrasolar Ring System: Indirect Evidence for Exosatellite Formation?

M.A. Kenworthy (1), E.E. Mamajek (2)

(1) Leiden Observatory, Leiden, The Netherlands, (2) University of Rochester, Rochester, NY, USA
 (kenworthy@strw.leidenuniv.nl)

Abstract

In May 2007, the young (16 million year) star 1SWASP J140747.93-394542.6 (“J1407”) underwent a complex series of eclipses that lasted 56 days, during which time it showed rapid variations of up to 50% in times of less than four hours. After ruling out other plausible alternatives, we conclude that there is an unseen secondary companion, J1407b, which hosts a giant ring system that fills a significant fraction of the Hill sphere. We present our exoring model, our search for J1407b, and discuss the future prospects for finding more of these systems in archival data.

1 The light curve

The young star 1SWASP J140747.93-394542.6 (“J1407”) is a 16-million-year-old pre-main sequence star in Scorpius-Centaurus OB Association (“Sco-Cen”), the nearest OB association. The SuperWASP and ASAS programs show that the star J1407 had a series of extremely complex eclipses over a two-month span in early 2007 (Mamajek et al. 2012), with $\sim 95\%$ of the star’s light blocked out near the minimum (see Figure 1). The star J1407 shows no evidence for accretion nor any circumstellar disk blueward of the WISE4 IR band, ruling out several simple hypotheses for these light curve fluctuations. Variability due to the presence of star spots and the star’s rapid rotation is seen at a level of 5% with a derived rotational period of 3.2 days (van Werkhoven et al. 2014).

2 Giant Exoring Model

We hypothesise that there is an unseen substellar companion J1407b (Kenworthy et al. 2015) in a near edge-on orbit to our line of sight. The eclipses have been modeled as due to a set of (at least 30) concentric dust

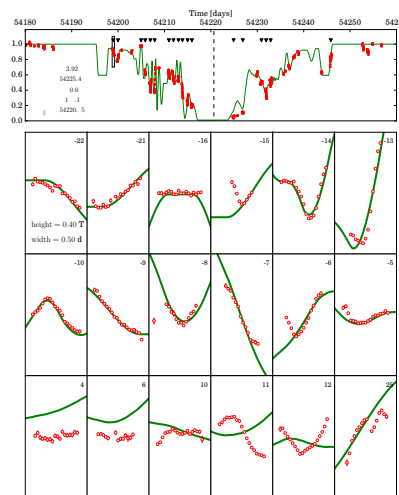


Figure 1: The lightcurve towards J1407.

rings with total mass of approximately 1 Earth mass, with radii ranging from approximately 30-90 million km (see Figure 2) that are in orbit around J1407b. Our non-detection of J1407b places strong upper limits on its mass with $20 - 40 M_{Jup}$ being the most likely range and with an orbital period of 10–30 years (Kenworthy et al. 2015). There is at least one very clean gap in the ring system at radius $\sim 0.4 AU$ which may be cleared by a sub-Earth-size exosatellite (see Figure 3; Mamajek et al. 2012; Kenworthy and Mamajek 2015). While popularly described as a “super-Saturn” with “rings”, given the age of the system, and the size and inferred mass of the rings, it seems plausible that we are detecting a circumplanetary (or protoexosatellite) disk. The disk would appear to fill a non-negligible fraction of its

Hill radius, and the appearance of gaps would suggest that system is in the process of spawning exosatellites.

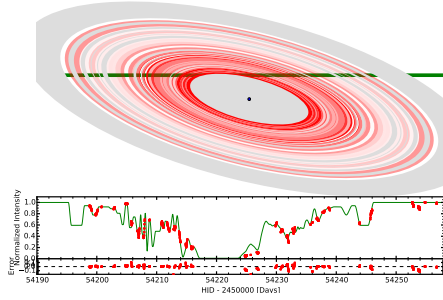


Figure 2: Ring model for J1407 lightcurve. The diameter of the rings is 1.6 AU. The green line shows the path of J1407b behind the ring system. Optical depth is represented by different shades of red. Grey areas indicate regions with no photometric coverage.

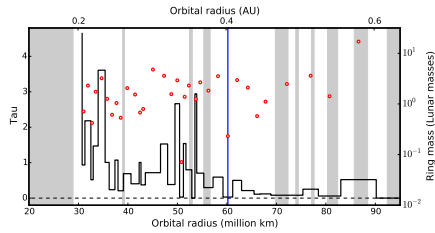


Figure 3: Optical depth versus radial distance from J1407b. The blue line indicates a ring cap clearing which we attribute to a Mars-mass exosatellite in orbit around J1407b. Grey areas indicate regions with no photometric coverage.

I will summarize the current knowledge about the J1407 system including archival and on-going photometric searches for additional eclipses, imaging and Doppler constraints on the companion of the ringed companion, and future prospects for discovering eclipsing disks girding young exoplanets and sub-stellar objects.

References

M. A. Kenworthy, S. Lacour, A. Kraus, A. H. M. J. Triaud, E. E. Mamajek, E. L. Scott, D. Ségransan, M. Ireland, et al. “Mass and period limits on the

ringed companion transiting the young star J1407”. *MNRAS* 446 (2015) 411–427. 1410.6577, [ADS].

M. A. Kenworthy and E. E. Mamajek. “Modeling Giant Extrasolar Ring Systems in Eclipse and the Case of J1407b: Sculpting by Exomoons?” *ApJ* 800 (2015) 126. 1501.05652, [ADS].

E. E. Mamajek, A. C. Quillen, M. J. Pecaut, F. Moolekamp, E. L. Scott, M. A. Kenworthy, A. Collier Cameron, and N. R. Parley. “Planetary Construction Zones in Occultation: Discovery of an Extrasolar Ring System Transiting a Young Sun-like Star and Future Prospects for Detecting Eclipses by Circumsecondary and Circumplanetary Disks”. *AJ* 143 (2012) 72. 1108.4070, [ADS].

T. I. M. van Werkhoven, M. A. Kenworthy, and E. E. Mamajek. “Analysis of ISWASP J140747.93-394542.6 eclipse fine-structure: hints of exomoons”. *MNRAS* 441 (2014) 2845–2854. [ADS].

NanoRocks: Studying Planet Formation and Planetary Rings on the International Space Station

Julie Brisset, Joshua Colwell, Adrienne Dove, Doug Maukonen, Nico Brown, Kelly Lai and Bradley Hoover

(1) Planetary Sciences Group, Department of Physics, University of Central Florida, 4000 Central Florida Blvd, Orlando FL 32816-2385, julie.brisset@ucf.edu

Abstract

We report on the initial results of the NanoRocks experiment on the ISS, which simulates collisions in protoplanetary disks and planetary ring systems. The objective of the NanoRocks experiment is to study low-energy collisions inside systems of multiple mm-sized particles of different shapes and materials. In September 2014, NanoRocks reached ISS as part of the NanoRacks platform. First video data from the experiment operations on ISS allows for the measurement of energy damping inside multi-particle systems and the observation of the formation of clusters.

1. Scientific Background

We report on the initial results of the NanoRocks experiment on the International Space Station (ISS), which simulates collisions that occur in protoplanetary disks and planetary ring systems. The standard model of planet formation proceeds from the gravitational collapse of an interstellar cloud of gas and dust through collisional accretion of solids into planetesimals and eventual runaway growth to form the terrestrial and giant planets [4]. A critical stage of that process is the growth of solid bodies from mm-sized chondrules and aggregates to km-sized planetesimals where gravity becomes an important force for further growth. Theories on this dust growth phase include gravitational instability ([3], [6]) and direct binary accretion of particles [5]. To characterize the collision behavior of dust in protoplanetary conditions, experimental data is required, working hand in hand with models and numerical simulations.

In addition, the collisional evolution of planetary rings takes place in the same collisional regime. Particles in Saturn's main rings collide at speeds on the order of 1 cm/s. The viscous evolution of the ring depends on the amount of energy dissipated in these

low energy collisions. With the age and origin of Saturn's rings remaining a major unknown in our understanding of the solar system, there is a critical need for fundamental data on the collisional interactions between particles in an environment like that of the rings (microgravity, with a regolith coating on larger particles). Clumping of particles in Saturn's rings has been observed by Cassini, illustrating that even in an environment where tidal forces inhibit gravitational aggregation, some accretion does occur in the form of self-gravity wakes [2].

2. The NanoRocks Experiment

The objective of the NanoRocks experiment is to study low-energy collisions of mm-sized particles of different shapes and materials. The low relative velocities required for these collisions can only be obtained under long-term microgravity conditions. The main component of this experiment is an aluminum tray (~8x8x2cm), which is divided into eight sample cells each holding different types and combinations of particles (i.e., glass, acrylic, copper, and rock). This tray is mounted on three springs to allow for its 3-dimensional shaking. During an experiment run, a magnet hits the bottom of the tray at regular time intervals to agitate the particle samples. The low-energy collisions generated by this shaking are recorded autonomously with a high-speed camera commanded by on-board electronics (Figure 1). Each experiment run consists of a 60 minute recording of the samples while they are being shaken once every minute.

In September 2014, NanoRocks reached ISS as part of the NanoRacks platform. Since its arrival, the experiment has been performing nominally, recording low-velocity collisions inside of the sample cells. About 10 experiment runs have been performed and 5 video files were downloaded from Station.

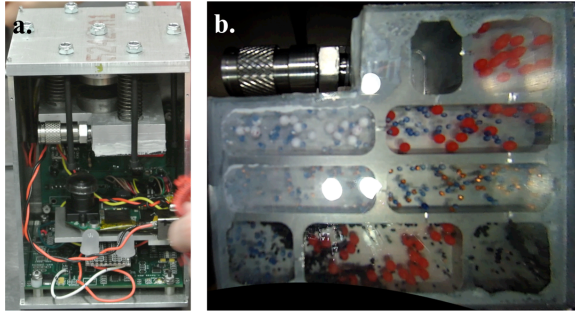


Figure 1: The NanoRocks experiment: a. Experiment hardware before closing: the camera and electronics can be seen at the bottom of the picture, while the tray and its springs and magnet are at the top. b. Recorded image of the experiment tray containing the eight particle samples during an experiment run on ISS.

3. First Data Results

First data analysis clearly shows the damping of the particle system “temperature” by inter-particle collisions that are not perfectly inelastic (Figure 2). The mean velocity evolution in the NanoRocks trays after each shaking event indicates a stochastic distribution of the coefficient of restitution [1]. The temporal evolution of the kinetic energy in the different many-particle systems can be measured.

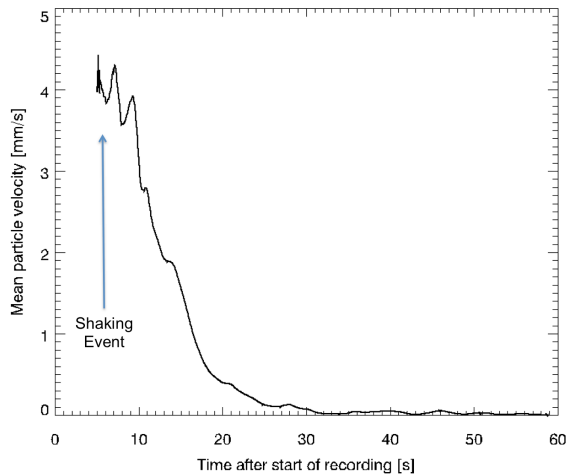


Figure 2: Mean particle velocity during and after a shaking event in one of the NanoRocks experiment cells. The damping of the system's energy through inter-particle collisions can clearly be recognized.

In addition, very low energy collisions in the NanoRocks many particle systems lead to the systematic formation of structures and clusters after a relaxation time following shaking events (Figure 3).

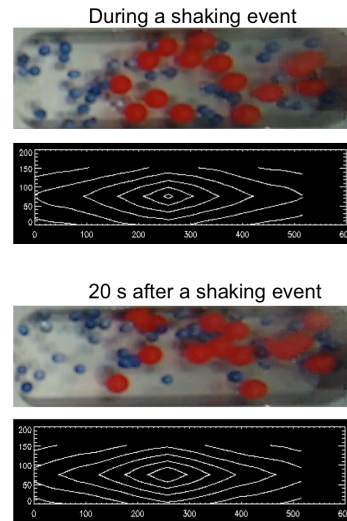


Figure 3: Particle clumping in one of the NanoRocks trays, during and 20 s after a shaking event. The contour levels of the auto-correlated images are shown under the originals (same contour levels) and indicate the mean clump size in the tray.

Acknowledgements

We would like to thank Space Florida for funding this work and the NanoRacks team for their support in operating the payload on Station and retrieving the scientific data.

References

- [1] Aspelmeier, T., Giese, G., Zippelius, A. *Physical Review E* 57, no. 1 (01 1998): 857-865.
- [2] Colwell, J. E., Esposito, L. W. and Sremcevic, M. *Geophysical Research Letters*, 33, no. 7 (04 2006).
- [3] Goldreich, Peter, and William R. Ward. *The Astrophysical Journal* 183 (1973): 1051-1062.
- [4] Klahr, Hubert, and Wolfgang Brandner. "Planet Formation." Edited by Hubert Klahr and Wolfgang Brandner. (Cambridge University Press) 05 2006.
- [5] Windmark, F., T. Birnstiel, C. Güttler, J. Blum, C. P. Dullemond, and Th. Henning. *Astronomy & Astrophysics* 540 (04 2012): 17.
- [6] Youdin, Andrew N., and Eugene I. Chiang. *The Astrophysical Journal* 601, no. 2 (02 2004): 1109-1119.

Simulating the librational behaviour of propeller moons in Saturn's rings

Michael Seiler, Martin Seiß, Holger Hoffmann, Ted Moldenhawer and Frank Spahn
Department of Physics and Astronomy, University of Potsdam, Germany (miseiler@uni-potsdam.de)

Abstract

Since its arrival at Saturn in 2004 the observations by the spacecraft Cassini have revolutionised the understanding of the dynamics in planetary rings. One of the tremendous discoveries of the Cassini space mission has been the detection of small disk-embedded moons in the dense rings of the Saturnian system. These small disk-embedded objects (*moonlets*) are not directly observable by the cameras aboard the spacecraft Cassini and cause S-shaped density variations in the surrounding ring material and therefore are called *propellers*.

Recurrent observations of the same propeller structures in Saturn's A ring allowed the reconstruction of their orbital motion from the Cassini ISS images and revealed a systematic sinusoidal excess motion from the expected Keplerian orbit of several 100 km in azimuthal direction [1]. Many attempts have been started to explain this librational behaviour, but none of them has been able to successfully explain all of the observed features [4, 2, 3, 6].

Resonant moon-moon interactions are well known phenomena in the Saturnian system and result in the same systematic librational behaviour as observed for the propellers [5, 1].

Therefore, here, we discuss the possibility that the observed periodical excess motion of the propellers is caused by the gravitational interaction with the moons of Saturn. We present results of N-body simulations where we integrate the orbital evolution of a moonlet - treated as a test particle - under the gravitational influence of one or more perturbing moons. We examine the resulting librational excess motion of the moonlet and identify a set of moons, which explains the observed libration frequencies and amplitudes. In our simulations we account for interactions between all relevant moons of the Saturnian system which automatically allows the consideration of many-body resonances.

Acknowledgements

This work was supported by the Deutsche Forschungsgemeinschaft (Sp 384/28-1, Sp 384/24-2) and the Deutsches Zentrum für Luft- und Raumfahrt (OH 1401).

References

- [1] Tiscareno, M. S. et al., Physical Characteristics and Non-Keplerian Orbital Motion of "Propeller" Moons Embedded in Saturn's Rings, *Astrophysical Journal Letters*, 718, pp. L92-L96, 2010
- [2] Pan, M. and Chiang, E., The Propeller and the Frog, *Astrophysical Journal Letters*, 722, pp. L178-L182, 2010
- [3] Pan, M. and Chiang, E., Care and Feeding of Frogs, *The Astronomical Journal*, 143, pp. 9, 2012
- [4] Rein, H. and Papaloizou, J. C. B., Stochastic orbital migration of small bodies in Saturn's rings, *Astronomy and Astrophysics*, 524, pp. A22, 2010
- [5] Spitale, J. N. et al., The Orbits of Saturn's Small Satellites Derived from Combined Historic and Cassini Imaging Observations, *The Astronomical Journal*, 132, pp. 692-710, 2006
- [6] Tiscareno, M. S., A modified 'Type I migration' model for propeller moons in Saturn's rings, *Planetary and Space Science*, 77, p. 136-142, 2013

Tribocharging and charged interaction in same-material, microscopic grains

S. Waitukaitis (1), V. Lee (2) and H. Jaeger (2)

(1) Leiden Institute for Physics, Leiden University, Leiden, The Netherlands (swaitukaitis@gmail.com)

(2) James Franck Institute and Department of Physics, The University of Chicago, Chicago, USA

Abstract

We experimentally address the causes and consequences of charging between same-material, microscopic grains. We confirm quantitatively that differences in grain size alone drive charging. By comparing our data to independent thermoluminescence measurements, we show that trapped electrons are not the charged species being transferred. We observe and quantify a zoology of interactions between grains, including attractive orbits and repulsive slingshot events, cluster growth and annihilation via collisions, and granular molecule formation. Our results highlight the important role played by grain polarizability in aggregation and have implications for the dynamics of dust particles in protoplanetary disks.

1. Introduction

The triboelectrification of microscopic grains is thought to be important in settings ranging from volcanic ash clouds [1] to protoplanetary disks [2, 3]. Perhaps the most perplexing aspect of this phenomenon is that it occurs between grains of the *same material*, a fact that violates our intuition that tribocharging should only occur between *different* materials. While this has been known for quite some time [4], and indeed models have been put forth to explain it [5], our understanding of how it works remains foggy at best owing to a lack of experimental data.

We have devised an experimental technique that addresses this gap. By observing a dilute stream of microscopic grains as they fall freely from an orifice in vacuum, we remove gravity and are able to access the otherwise hidden electrostatic forces. Subjecting the grains to a uniform horizontal electric field, we are able to extract the granular charge distribution and for the first time quantify the scale of charge transfer in same material grains. We compare this to independent thermoluminescence measurements and rule out trapped electrons as the species being transferred.

Finally, removing the field we are able to watch the grains as they interact amongst themselves. This allows us to witness attractive orbits and repulsive slingshot events, cluster growth and annihilation and granular molecule formation—processes of immediate relevance to planet formation.

2. Charge Measurements

We use an experimental technique similar to Millikan to measure the charges of individual grains [6], but with an adaptation to work with much larger grains and much smaller charge-to-mass ratios. Full details can be found in our previous work [7, 8]. In brief, we subject the grains to a uniform horizontal electric field as they fall vertically in high vacuum. Capturing their motion with a co-falling high speed camera (Phantom v9.1) allows us to track their motion. By fitting the horizontal position of each grain to a parabola, we extract its acceleration. With knowledge of the average grain mass (measured independently by microscopy) we translate the acceleration measurement into a charge measurement. This technique offers a charge-to-mass resolution of $\sim 5 \times 10^5$ elementary charges and a force resolution of ~ 500 pN (comparable to an atomic force microscope).

We work with highly spherical samples of fused zirconium dioxide-silicate grains ($\text{ZrO}_2\text{:SiO}_2$ with mass fraction $\sim 65:35$) because they are readily available, known to charge well, and known for being capable of holding trapped electrons. (This last point is important because trapped electrons have been considered the leading candidate for the charge species being transferred in same material tribocharging [9].) For monodisperse samples (average diameter $\bar{d} = 300 \pm 9 \mu\text{m}$) we typically find a mean charge close to zero ($\sim 10^4$ elementary charges per grain) and a much larger width ($\sim 10^6$ elementary charges). The scale of the charge distribution width indicates that charging is *not* driven by thermal fluctuations, which would be commensurate with a much smaller width [7].

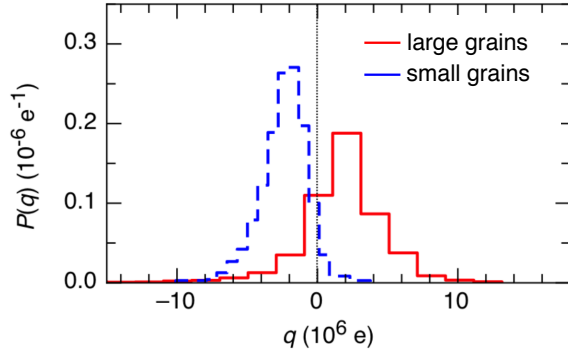


Figure 1: (a) Example still from a high speed video of a monodisperse sample. (b) Charge distributions for binary-sized sample comprised of 50:50 (by number) of large (average diameter $\bar{d}_l = 326 \pm 10 \mu m$) and small ($\bar{d}_s = 251 \pm 10 \mu m$) grains.

When we mix two well-separated sizes of grains together, we find that the grains exchange electrical charge with the larger ones becoming positive and the smaller ones negative [8]. Typical data is shown in Fig. 1. This confirms qualitative measurements made previously [10], but here we are able to measure that the amount of charge being transferred is, on average, $\sim 10^6$ elementary charges. By independently measuring the density of trapped electrons with thermoluminescence, we find that there far too few to account for the observed charge transfer [8].

3. Charged Interactions

In the absence of any external field, the grains are free to interact with each other as they fall. Again using the high speed camera, we can observe, quantify, and categorize these interactions. The behaviors we see are qualitatively different for monodisperse and bidisperse samples. This difference arises from the different charge distributions in the two cases.

For monodisperse grains, we see a variety of long range charged interactions. These are explained in detail in our forthcoming manuscript [11] and include attractive elliptical orbits with bounces and attractive and repulsive hyperbolic orbits. By measuring the sizes of grains in the video and fitting segments of these orbits, we are able to extract the charges of pairs of particles on a case by case basis (see Fig. 2a for an example orbital path with bounces). Typically we find that the grains exhibiting such behavior are drawn from the tails of the monodisperse charge distribution, with absolute charges on the order of $10^6 e$. We also

observe cluster growth and annihilation events where groups of particles grow or are disrupted after colliding with an incoming particle.

Perhaps surprisingly, for bidisperse grains we see *less* long range charged interactions. Instead, we see stable *granular molecules*—groups of large and small particles stuck together with conspicuously characteristic geometries. This is presumably because the larger amount of charge exchange leads to stronger interactions that more quickly damp out any initial motion. An example molecule consisting of five large particles and one small one is shown in Fig. 2b. Given that the binary samples charge systematically, we can assume the small grains have charge $-q$ and the large grains charge $+q$ with high likelihood (where q represents the average amount of charge transferred between the large and small grains—see [11]). Using this knowledge in combination with the full interaction potential (including the Coulomb interaction, polarization effects and steric repulsion), we are able to predict the shapes of such molecules.

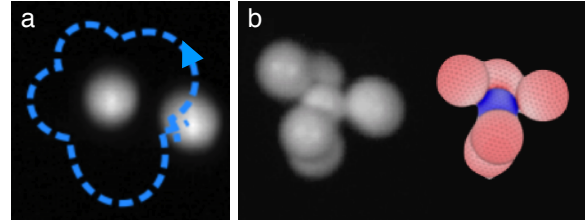


Figure 2: (a) Bouncing orbital path of an oppositely charged pair of grains from a monodisperse sample. (b) Example granular molecule from bidisperse experiments (left) and simulated counterpart (right) that form when one negatively-charged small particle is surrounded by five positively-charged large particles.

4. Summary and Conclusions

We have shown that same material grains transfer electrical charges between each other and that the driving mechanism is related to grain size. Our measurements of the amount of charge transferred reveal that it is too large to be accounted for by trapped electrons. Finally, we are able to observe the interactions of these charged grains in detail, which may play an important part in the aggregation dynamics of protoplanetary disks.

Acknowledgements

We thank Edward Barry, Ray Cocco, Karl Freed, Daniel Lacks, Kieran Murphy, Sid Nagel, Ivo Peters, Jian Qin, John Royer, and Tom Witten for insightful discussions. S. R. W. acknowledges support from a University of Chicago Millikan Fellowship and from Mrs. Joan Winstein through the Winstein Prize for Instrumentation. This research was supported by NSF through DMR-1309611. The Chicago MRSEC, supported by NSF DMR-1420709, is gratefully acknowledged for access to its shared experimental facilities.

References

- [1] R. Anderson, *et al.*, Science Vol. 148, pp. 1179, 1965.
- [2] T. Poppe, J. Blum, T. Henning, Astrophysical Journal, Vol. 533, pp. 472-480, 2000.
- [3] J. Blum and G. Wurm, Annual Review of Astronomy and Astrophysics, Vol. 46, pp. 21-56, 2008.
- [4] P. Shaw, Nature, Vol. 118, pp. 659-660, 1926.
- [5] D. Lacks, N. Duff and S. Kumar, Physical Review Letters, Vol. 100, 188305, 2008.
- [6] R. Millikan, Physical Review, Vol. 32, pp. 349-397, 1911.
- [7] S. Waitukaitis and H. Jaeger, Review of Scientific Instruments, Vol. 84, 025104, 2013.
- [8] S. Waitukaitis, V. Lee, J. Pierson, J. Forman and H. Jaeger, Physical Review Letters, Vol. 112, 218001, 2014.
- [9] J. Lowell and W. Truscott, Journal of Physics D, Vol. 19, pp. 1273, 1986.
- [10] K. Forward, D. Lacks, and R. Sankaran, Physical Review Letters, Vol. 102, 028001, 2009.
- [11] V. Lee, S. Waitukaitis, M. Miskin and H. Jaeger, *in review with Nature Physics*.

In situ dust measurements by the Cassini Cosmic Dust Analyzer in 2014 and beyond

R. Srama (1,2) and the CDA Science Team

(1) Institute of Space Systems, IRS, Univ. Stuttgart, Ger (rsrama@irs.uni-stuttgart.de) (2) Baylor Univ., Waco, TX, USA

Abstract

Today, the German-lead Cosmic Dust Analyser (CDA) is operated continuously for 11 years in orbit around Saturn. Many discoveries like the Saturn nanodust streams or the large extended E-ring were achieved. CDA provided unique results regarding Enceladus, his plume and the liquid water below the icy crust. In 2014 and 2015 CDA focuses on extended inclination and equatorial scans of the ring particle densities. Furthermore, scans are performed of the Pallene and Helene regions. Special attention is also given to the search of the dust cloud around Dione and to the Titan region. Long integration times are needed in order to characterize the flux and composition of exogenous dust (including interstellar dust) or possible retrograde dust particles. Finally, dedicated observation campaigns focus on the coupling of nanodust streams to Saturn's magnetosphere and the search of possible periodicities in the stream data. Saturn's rotation frequency was identified in the impact rate of nanodust particles at a Saturn distance of 40 Saturn radii.

A special geometry in 2014-065 lead to an occultation of the dust stream by the moon Titan and its atmosphere when Titan crossed the line-of-sight between Saturn and Cassini. Here, CDA pointed towards Saturn for the measurement of stream particles. Around closest approach when Cassini was behind Titan, the flux of stream particles went down to zero (Fig. 1). This „dust occultation“ is a new method to analyse the properties of the stream particles (speed, composition, mass) or the properties of Titans atmosphere (density). Furthermore, the particle trajectories can be constrained for a better analysis of their origin.

In the final three years CDA performs exogenous and interstellar dust campaigns, studies of the composition and origin of Saturn's main rings by unique ring ejecta measurements, long-duration

nano-dust stream observations, high-resolution maps of small moon orbit crossings, studies of the dust cloud around Dione and studies of the E-ring interaction with the large moon Titan.

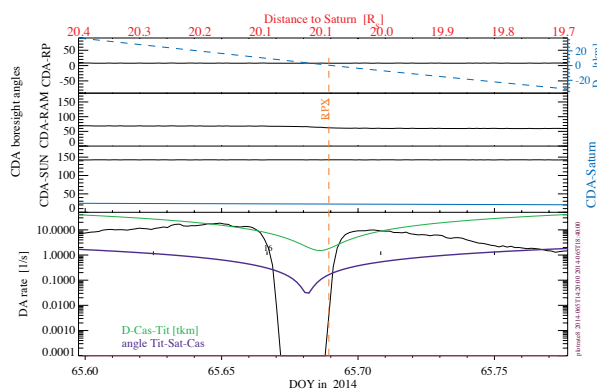


Fig. 1 Angles between the CDA boresight and various objects/directions (Sun, RingPlane, DustRAM, Sun, Saturn, top diagrams) and the dust impact rate (bottom). The flux of stream particles stopped behind the moon Titan around 2014-065T16:40.

Intrinsic structure in Saturn's rings

N. Albers

University of Colorado at Boulder, LASP, Boulder, CO, USA (Nicole.Albers@lasp.colorado.edu)

Abstract

Saturn's rings are the most prominent in our Solar system and one example of granular matter in space. Dominated by tides and inelastic collisions the system is highly flattened being almost 300000km wide while only tens of meters thick. Individual particles are composed of primarily water ice and range from microns to few tens of meters in size. Apparent patterns comprise ringlets, gaps, kinematic wakes, propellers, bending waves, and the winding spiral arms of density waves. These large-scale structures are perturbations foremost created by external as well as embedded moons.

Observations made by the Cassini spacecraft currently in orbit around Saturn show these structures in unprecedented detail. But high-resolution measurements reveal the presence of small-scale structures throughout the system. These include self-gravity wakes (50-100m), overstable waves (100-300m), sub-km structure at the A and B ring edges, "straw" and "ropy" structures (1-3km), and the C ring "ghosts". Most of these had not been anticipated and are found in perturbed regions, driven by resonances with external moons, where the system undergoes periodic phases of compression and relaxation that correlate with the presence of structure. High velocity dispersion and the presence of large clumps imply structure formation on time scales as short as one orbit (about 10 hours).

The presence of these intrinsic structures is seemingly the response to varying local conditions such as internal density, optical depth, underlying particle size distribution, granular temperature, and distance from the central planet. Their abundance provides evidence for an active and dynamic ring system where aggregation and fragmentation are ongoing on orbital timescales. Thus a kinetic description of the rings may be more appropriate than the fluid one.

I will present Cassini Ultraviolet Spectrometer (UVIS) High Speed Photometer (HSP) occultations, Voyager 1 and 2 Imaging Science Subsystem (ISS), and high-resolution Cassini ISS images. I will discuss the kinematics of the A and B ring edges and their deviations from their expected $m=2$ and $m=7$ lobed pat-

terns, show wavelet signature and morphology of sub-km structure found at these edges and in strong density waves, and illustrate observed characteristics of the C ring "ghosts" as well as self-gravity wakes in the A and B ring.

Finally I will review our current theoretical understanding of the small-scale structure and size distribution of Saturn's rings with respect to particle-particle collisions, aggregate stability, and kinetic modeling.

Acknowledgements

This work is supported by the Cassini project.

A new moon-induced structure

N. Albers, M. Sremčević, and L.W. Esposito

University of Colorado at Boulder, LASP, Boulder, CO, USA (Nicole.Albers@lasp.colorado.edu)

Abstract

Embedded moons are known to create an observable propeller-shaped structure in the surrounding ring which consists of a gap and kinematic wake. In the cases of Pan and Daphnis, the moons are sufficiently massive to open a circumferential gap - the Encke and Keeler gap, respectively. New results, however, reveal the existence of a previously unknown moon-associated structure found at the Encke and Keeler gap edges.

By analyzing Cassini Ultraviolet Spectrometer (UVIS) High Speed Photometer (HSP) and Voyager 2 Photopolarimeter (PPS) occultations we found a few kilometer wide gaps located within a few kilometers of the ring edges. These transparent regions feature sharp edges and have so far been found exclusively downstream of the respective embedded moon. Gap characteristics for features found near the inner and outer Encke gap edges are consistent with each other. Two occultations with special observing geometries, one tracking and one double-star, allow to investigate spatial and temporal morphology of these gaps. Our preliminary results suggest that these structures are individual gaps with an aspect ratio of about 1:5 and may thus be about 10km long.

Their existence offers another avenue in searching for embedded objects although our preliminary search did not produce examples apart from those reported here for Pan and Daphnis.

Acknowledgements

This work is supported by the Cassini project.

Breakage of the energy equipartition and aggregate formation in sheared system

Y. Baibolatov and F. Spahn

University of Potsdam, Germany (14476 Potsdam, Germany, Karl-Liebknecht Str 24-25)

Abstract

In classical thermodynamics any mixture of gases with different masses with any sort of initial temperature differences tend to relax into a stationary state with a unique temperature along the whole system. But this is not true in case of granular mixtures, where energy is dissipated during each collision between particles. As a result, in a granular mixture of species with different masses, the system does not have a unique thermodynamic temperature but each species has its own temperature. This effect has been paid much attention recently [1, 2, 3]. Apart from the dissipative particle interaction, the main reason for this behaviour is due to the mass difference of the colliding particles, causing an asymmetric energy loss of particles. The loss of energy can be compensated by external heating of the system. In the case of planetary rings system, the role of heating is played by gravitational shear caused by the planet.

In this work we consider the model consisting of identical spherical and adhesive particles. Although the constituents are identical, they can form aggregates and effectively create particles with larger masses. The differences in masses lead to different velocity dispersions (granular temperatures) of the aggregates. This interplay between heat transfer among aggregates and the distribution of the aggregate sizes under the gravitational shear is of crucial importance for the formulation of mean-field balance equations for the ring particle ensembles.

- [3] Uecker, H., Kranz, W.T., Aspelmeier, T. and Zippelius, A.: Partitioning of energy in highly polydisperse granular gases, *Physical Review E*, Vol. 80, p. 041303, 2009.

References

- [1] Bodrova, A., Levchenko, D., and Brilliantov, N.: Universality of temperature distribution in granular gas mixtures with a steep particle size distribution, *EPL*, Vol. 106, p. 14001, 2014.
- [2] Barrat, A., and Trizac, E.: Lack of energy equipartition in homogeneous heated binary granular mixtures, *Granular Matter*, Vol. 4, pp. 57-63, 2002.